

General Disclaimer

One or more of the Following Statements may affect this Document

- This document has been reproduced from the best copy furnished by the organizational source. It is being released in the interest of making available as much information as possible.
- This document may contain data, which exceeds the sheet parameters. It was furnished in this condition by the organizational source and is the best copy available.
- This document may contain tone-on-tone or color graphs, charts and/or pictures, which have been reproduced in black and white.
- This document is paginated as submitted by the original source.
- Portions of this document are not fully legible due to the historical nature of some of the material. However, it is the best reproduction available from the original submission.

(NASA-TM-X-73621) RESULTS OF CLOSED CYCLE
MHD POWER GENERATION TEST WITH A
HELIUM-CESIUM WORKING FLUID (NASA)
A02/HP A01

10 p HC
CSCL 20I

N77-23936

63/75
Unclas
29071

**NASA TECHNICAL
MEMORANDUM**

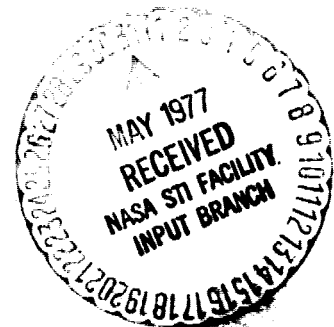
NASA TM X-73621

NASA TM X-73621

**RESULTS OF CLOSED CYCLE MHD POWER GENERATION
TEST WITH A HELIUM-CESIUM WORKING FLUID**

by Ronald J. Sovie
Lewis Research Center
Cleveland, Ohio 44135

**TECHNICAL PAPER to be presented at the
16th Symposium on the Engineering Aspects
of Magnetohydrodynamics
Pittsburgh, Pennsylvania, May 16-18, 1977**



RESULTS OF CLOSED CYCLE MHD POWER GENERATION TESTS WITH A HELIUM-CESIUM WORKING FLUID

Ronald J. Sovie
NASA Lewis Research Center
Cleveland, Ohio

Abstract

The cross-sectional dimensions of the MHD channel in the NASA Lewis closed loop facility have been reduced to 3.8x11.4 cm. Tests were run in this channel using a helium-cesium working fluid at stagnation pressures of 1.5×10^5 N/M², stagnation temperatures of 2000-2060K and an entrance Mach number of 0.36. In these tests Faraday open circuit voltages of 200V were measured which correspond to a Faraday field of 1750 V/M. Power generation tests were run for different groups of electrode configurations and channel lengths. Hall fields up to 1450 V/M were generated. Power extraction per electrode of 183W and power densities of 1.7 MW/M³ have been obtained. A total power output of 2 kW was generated for tests with 14 electrodes. The power densities obtained in this channel represent a factor of 3 improvement over those reported for the M = 0.2 channel at the last EAM Symposium.

I. Introduction

Closed cycle MHD power generation systems appear to have excellent potential for use as lightweight space power systems¹ and more efficient terrestrial power plants^{2,3,4}. In the latter case the heat source for the MHD power system could be an advanced gas cooled reactor, a fusion reactor⁵, a fossil fuel fired combustion heat exchanger^{4,6}, or perhaps even a solar heat source. The realization of this potential requires that efficient, long-lived MHD generators and system components be developed. The experimental closed cycle MHD program at Lewis addresses the lifetime and systems aspects of this development.

The goal of the NASA Lewis closed cycle MHD program is to demonstrate non-equilibrium MHD performance at power densities of 10-20 MW/M³ initially for periods of minutes and ultimately for 100's of hours in a realistic environment. The experiments are performed in a closed-loop, steady-state facility with hot generator walls to better simulate the conditions under which a real generator must perform. This program complements the shock-tube programs aimed at demonstrating large enthalpy extraction ratios and reasonable turbine efficiencies^{7,8} and can supply much basic system and design information useful for both future longer duration blowdown experiments^{9,10} and possible future steady-state power systems.

In the program at Lewis we have overcome many of the problems associated with the successful operation of a steady-state facility at temperatures of 2000-2060K. Experiments have been performed using various working fluids at a variety of operating conditions. The MHD generator performance has steadily increased in the past few years although we have not as yet obtained any non-equilibrium MHD performance. Consequently, we have been decreasing the MHD channel dimensions to allow operation at higher

Mach numbers and increase the probability of obtaining non-equilibrium performance. The purpose of this paper is to describe the results of tests in the 3.8x11.4 cm MHD channel with a helium-cesium working fluid at M = 0.36.

II. Facility

Facility Operation

The overall design and operation of the closed loop MHD facility has been discussed previously^{11,12}. The only major modification made since the paper¹³ at the Fifteenth EAM Symposium was to reduce the channel cross-sectional dimensions from 5x16.5 cm to 3.8x11.4 cm. We were not able to incorporate facility modifications to further isolate the heater from ground since the last Symposium. Consequently, the voltage of the heater to ground is still limited to ~ 550V at peak temperatures during seed injection tests. Modifications to remedy this problem are presently underway, however.

The cesium seed injection tests are still run in either the normal mode or the blowdown mode. In the normal mode a monitored liquid cesium flow is continuously injected into the cesium storage plenum and injection system located in the heater. In the blowdown mode the liquid cesium is injected into the storage plenum and then blown out after a short duration using high pressure helium.

MHD generator tests are run under a variety of load conditions using either all 28 electrode pairs along the $l = 68.5$ cm channel length or using configurations in which some electrodes are loaded (i.e., 1-17, or 14-28), while the remaining electrodes are open circuited. In these latter electrode configurations, the magnetic field region in the open circuited part of the channel increases the Hall leakage resistance and allows for better performance. The decrease in the measured voltages at the open circuited electrodes from those measured when all the electrodes are open circuited can also be used to determine the value of the Hall leakage current¹³. This information is necessary because simultaneous measurement of the Faraday current, Hall voltage, and Hall leakage current is necessary in order to determine the vapor seed fraction, Sv, using the data analysis theory in ref. 14. The theory used is an extension of the results of Dzung¹⁵ and includes the effects of finite electrode segmentation, electrode voltage drops, and leakage resistances in the Hall and Faraday directions.

Operating Conditions

The operating conditions for the results presented herein were in the following ranges.

gas stagnation temperature, T_s , 2000-2060K
gas stagnation pressure, P_s , $1.5 \times 1.6 \times 10^5$ N/M²
helium mass flow, M_{He} , 0.14-0.16 Kg/s

B-9112

ORIGINAL PAGE IS
OF POOR QUALITY

Mach number, M, 0.34-0.37
gas velocity, μ , 920-940 m/s
impurity fraction, 50-100 ppm CO

In the initial tests made with this channel the Mach number was essentially constant along the channel length under no load conditions. This is shown by the data labeled Run 461 on figure 1. The Mach number profile as determined from static pressure measurements made at 15.4 cm intervals, along the channel length is shown on this figure. The data labeled Run 526 represent the Mach number profile for the last and highest temperature tests made in this channel. The figure shows that there is about a 5% increase in the Mach number in the region between electrodes 15 and 21. The open circuit voltage profile indicates that this change occurs right at electrode 21. The cause of this rather abrupt change is probably a canted brick when the system is at peak temperature.

Expected Performance

Since we have not as yet obtained non-equilibrium performance, the expected equilibrium performance for $T_s = 2060K$ and $B = 1.8 T$ is shown on figure 2. In this figure the power/electrode, Faraday current, I_f , and Hall field, E_x , are plotted versus cesium vapor seed fraction, S_v , for various values of the load resistance, R_L . The figure shows that we could expect ~ 300 W/electrode pair at $R_L = 30 \Omega$ and that the generated Hall fields would be quite large, i.e., ~ 2000-3000 V/M. The effect of a ground loop or Hall leakage resistance, R_x , on the expected equilibrium performance is shown on figure 3. The figure shows that if R_x is above 500 Ω , we can expect to obtain a reasonable fraction of the ideal equilibrium performance. The presence of an internal resistance in the Faraday direction, R_y , due to boundary layer and electrode effects, would lower the measured short circuit current and Hall field in the same manner as increasing the load R_L does in figure 2. The power/electrode would be reduced by the amount $I^2 R_y$, i.e., the power dissipated in this resistance.

We should expect significant non-equilibrium performance even at our relatively low Mach number and CO impurity concentration. The impurity fraction for the data presented herein was in the range $0.5-1 \times 10^{-4}$ (50-100 ppm) of CO. In figure 4 the expected conductivity for our geometry and non-equilibrium performance is plotted versus CO impurity fraction with the load factor as a parameter. The figure shows that the CO concentration has little effect unless it exceeds 10^{-3} .

The expected non-equilibrium performance at our run conditions is shown in figure 5. In this figure the power/electrode is presented as a function of load factor for a pair of CO fraction values. The figure shows that even at our relatively low Mach numbers we should obtain substantial increases over the equilibrium values presented in figure 2.

III. Experimental Results

Faraday Open Circuit Voltage Behavior

The variation of the measured Faraday open circuit voltage, V_{FOC} , along the channel length is shown in figure 6 for tests 461 and 526. The 461 test is one of the first tests run with this channel and the profile is essentially identical to that obtained in previous channels. The measured voltage rises to a peak value in the first nine or so electrodes and then remains essentially constant for the rest of the channel. The lower voltages in the channel entrance region are caused by the presence of pre-ionizer electrodes which partially short out the generated voltages. Run 526 represents the data taken in the final set of tests in this channel at temperatures of 2060K. In these tests the generated voltage reach a peak value at the 21st electrode pair in the region of increased Mach number.

The variation of the ratio of the measured V_{FOC} to the ideal $\mu B h$ along the channel length is shown for the same two cases in figure 7. The figure shows that in the initial tests typified by Run 461, the measured voltages were above 90% of the ideal for most of the channel. In the higher temperature tests (Run 526) the voltages do not exceed 90% of the ideal until about halfway down the channel. The values then approach the ideal. The Mach number variation was, of course, taken into consideration in the calculation of the ideal values. The figure shows that there was some deterioration in the Faraday leakage resistance values in the first part of the channel as we ran at higher temperatures.

Behavior at Short Circuit and Load Conditions

Tests were run for various seed injection methods, electrode configurations, and load resistances. The magnetic field strength, B , was 1.8 T for most tests. Representative data and results for the helium-cesium tests at $T_s = 2060K$ are given in Table I. The vapor seed fraction, S_v , boundary layer and electrode resistance, R_y , and Hall leakage resistance, R_x , have been calculated using the data analysis theory. The load factor K is $V_f / \mu B h$ and the effective load factor, K_{eff} , is defined as $K_{eff} = \frac{V_f + I_f R_y}{\mu B h}$. The power

output quoted in Table I for the $R_L = 0$ cases is the equivalent power, $\frac{1}{\mu} V_{FOC} I_{K=0}$. Where $I_{K=0}$ is

the current measured with no external load in the circuit. We use this equivalent power as a figure of merit for our generator since most of our runs are at short circuit conditions to enhance the probability of obtaining non-equilibrium. The power dissipated in the R_y resistances is not included in the power density values in Table I. This power is roughly ~ 100W/electrode pair for most of the cases run. The data in Table I typifies the behavior obtained in all the tests run.

The short circuit current profile for the 1-17 electrode configuration (Run 540) is shown in figure 8. The figure shows that the current decays after the front entrance end effect and then remains at the level 1.8-2.2 A. There are no non-equilibrium effects exhibited by the data. In the tests using the last half of the channel, the currents were generally higher and the profiles were more irregular due to the increase in Mach number in the latter quarter of the channel.

The data in Table I shows that power outputs of 125-136 W/electrode pair have been generated under load conditions using the blowdown seed injection. Equivalent powers and power densities of 183 W/electrode pair and 1.68 MW/M³ have been obtained. The performance difference between the normal and blowdown seed tests is illustrated by the run 537 data. The vapor seed fraction is lower under normal seed conditions and the power output is about half that obtained under blowdown conditions. The expected equilibrium power is lower at the lower seed rate, but the performance is also limited by a higher R_y for the normal seed injection.

The R_y values for most of the blowdown tests are in the range 18-25 Ω , and thus even at short circuit conditions K_{eff} is ~ .3-.4. It was shown in figure 5, however, that we could expect substantial non-equilibrium effects at these effective load parameters.

The Hall leakage resistance values vary from test to test, but in general they are higher for the tests using the latter half of the channel. Hall fields up to 1467 V/M have been generated for tests using electrodes 17-28 whereas they are in the range 700-900 V/M for the first part of the channel. The channel is presently being disassembled for inspection to determine the cause of this variation. Total power outputs up to 2.2 kW have been obtained for the tests shown in Table I. The maximum power output was 2.8 kW for a 28 electrode test.

IV. Discussion and Concluding Remarks

The area of the MHD channel was reduced to 3.8x11.4 cm to allow operation at higher Mach numbers. In tests run at $M = 0.36$ and $T_s = 2060K$, power densities up to 1.7 MW/M³ were obtained. This represents a factor of ~ 3 improvement over the results obtained in the previous $M = 0.2$ tests. The main reason for this increase is that the expected equilibrium power output is significantly increased at the higher Mach number. No non-equilibrium effects have been observed. The performance is limited by an effective boundary layer and electrode resistance of ~ 18-25 Ω and Hall leakage resistances that are in the range 100-400 Ω for most tests. Both these effects lower the current density and hence the probability of obtaining non-equilibrium.

In order to improve the MHD generator performance and better understand the phenomena occurring in the generator, a number of changes are

being incorporated into the facility. The heater wiring system, water cooling system, and the electrical isolation of the heater front end expansion joint are being modified to greatly increase the resistance of the heater to ground at the peak operating conditions. The MHD channel is being disassembled and will be inspected for potential shorting areas. The internal dimensions of the channel will then be further modified to achieve improved performance.

V. REFERENCES

1. Seikel, G. R., and Nichols, L. D., "The Potential of Nuclear MHD Electric Power Systems," AIAA Paper No. 71-636, presented at 7th Propulsion Joint Specialist Conference, Salt Lake City, Utah, June 14-18, 1971.
2. "Comparative Evaluation of Phase I Results from the Energy Conversion Alternatives Study (ECAS)---Coal Utilization for Electric Power Plants Feasibility Analysis," NASA TM X-71855 (Feb. 1976).
3. Seikel, G. R., et al., "A Summary of the ECAS Performance and Cost Results for MHD System," Proceedings of the 15th Symposium on the Engineering Aspects of Magnetohydrodynamics. B. Zauderer, ed., Mississippi Univ. Press, 1976, pp. III.4.1-III.4.22.
4. Zauderer, B. "Systems Studies of Coal Fired Closed Cycle MHD for Central Station Power," Proceedings of the 15th Symposium on the Engineering Aspects of Magnetohydrodynamics. B. Zauderer, ed., Mississippi Univ. Press, 1976, pp. III.5.1.-III.5.11.
5. Rosa, R. J., "Fusion Power Plants using Minimum Activity Blankets and MHD Conversion," Sixth International Conference on Magneto-hydrodynamic Electrical Power Generation, Intern. Atomic Energy Agency, Vienna, 1975, Vol. IV, pp. 69-99.
6. Cook, C. S., "Current Experimental Results from Operation of a Closed Cycle Ceramic Regenerative Heat Exchanger," Proceedings of 15th Symposium on the Engineering Aspects of Magnetohydrodynamics. B. Zauderer ed., Mississippi Univ. Press, 1976, pp. VIII.4.1.-VIII.4.5.
7. Tate, E., Marston, C. H., and Zauderer, B., "Large Enthalpy Extraction Results in a Non-Equilibrium MHD Generator," Sixth International Conference on Magnetohydrodynamic Electrical Power Generation, Internl. Atomic Energy Agency, Vienna, 1975, Vol. III, pp. 89-104.
8. Blom, J., et al., "High Power Density Experiments in the Eindhoven Shock Tunnel MHD Generator," Sixth International Conference on Magnetohydrodynamic Electrical Power Generation, Internl. Atomic Energy Agency, Vienna, 1975, Vol. III, pp. 73-88.

ORIGINAL PAGE IS
OF POOR QUALITY

9. Zauderer, B., et al., "Blowdown Test Facility for a Fossil Fueled Nonequilibrium MHD Generator," Proceedings of the 13th Symposium on the Engineering Aspects of Magnetohydrodynamics, M. Mitchner, ed., Mississippi Univ. Press, 1973, pp. IV.3.1.-IV.3.-6.
10. Rietjens, L. H. Th., "Summary of Closed Cycle MHD Research at Eindhoven University of Technology," Closed Cycle MHD Power Generation, NASA TM X-71848, R. J. Sovie ed., 1975, pp. 25-26.
11. Sovie, R. J., and Nichols, L. D., "Status of Power Generation Experiments in the NASA Lewis Closed Cycle MHD Facility," AIAA Paper No. 72-103, presented at 10th Aerospace Sciences Meeting, San Diego, California, January 17-19, 1972.
12. Sovie, R. J. and Nichols, L. D., "Closed Cycle Power Generation Experiments in the NASA Lewis Facility," Proceedings of the 14th Symposium on the Engineering Aspects of Magnetohydrodynamics. Y.C.L. Wu, ed., Mississippi Univ. Press, 1974, pp. VII.6.1-VII.6.6.
13. Sovie, R. J. "Closed Cycle MHD Power Generation Experiments Using a Helium-Cesium Working Fluid in the NASA Lewis Facility," Proceedings of the 15th Symposium on the Engineering Aspects of Magnetohydrodynamics. B. Zauderer ed., Mississippi Univ. Press, 1976, pp. VI.1.1-VI.1.6.
14. Nichols, L. D. and Sovie, R. J., "Hall Current Effects in the NASA Lewis Magnetohydrodynamic Generator," NASA TM X-2606 (Jul. 1972).
15. Dzung, L. S., "Influence of Wall Conductance on the Performance of MHD Generators with Segmented Electrodes," Symposium on Magnetohydrodynamic Electrical Power Generation; Electricity From MHD, International Atomic Energy Agency, Vienna, 1966, Vol. II, pp. 169-176.

ORIGINAL PAGE IS
OF POOR QUALITY

TABLE 1. - TYPICAL RESULTS FOR HELIUM CESIUM TESTS
 [Run conditions $T_S \approx 2060$ K, $P_H \approx 1.6 \times 10^{-5}$ N/M², $m_{HE} = 0.15$ kg/s, $M \approx 0.36$.]

Run no.	Remarks	Magnetic field strength B, T	Electrode configuration	Load resistance, R _L , Ω	Load factor, K	Faraday current, I _y , A	Power			Hall voltage, V	Hall field, V/M	Cesium vapor seed fraction, S _v , %	Boundary layer and electrode resistance, R _y , Ω	Hall leakage resistance, R _x , Ω	Effective load factor, K _{EFF}
							Per electrode, M	Total output, kW	Density, MM/M ³						
540	a, b	1.8	1-17	0	0	2.2	72	1.22	0.66	310	747	0.65	41.8	110	0.61
519	b	1.8	14-28	30	0.27	2.08	130	1.95	1.19	270	737	0.68	23.6	261	0.515
536	a, b	1.8	14-28	0	0	2.92	135	2.03	1.24	320	886	0.79	22.8	88	0.333
537	c	1.8	15-28	30	0.23	1.45	63	0.83	0.58	310	907	0.23	43.8	227	0.54
537	b	1.8	15-28	30	0.3	2.04	125	1.75	1.15	220	644	0.81	18.8	103	0.49
526	a, b	1.83	17-28	0	0	3.7	183	2.2	1.68	430	1467	0.6	19.1	399	0.35
527	b	1.84	17-28	30	0.28	2.07	120	1.55	1.18	310	1058	0.37	24.7	466	0.54
529	b	1.81	17-28	60	0.45	1.51	136	1.63	1.25	220	750	0.37	24.7	289	0.64

^aPower is defined as $1/4 V_{FOC} I_K = 0$.
^bBlowdown seed injection.
^cNormal seed injection.

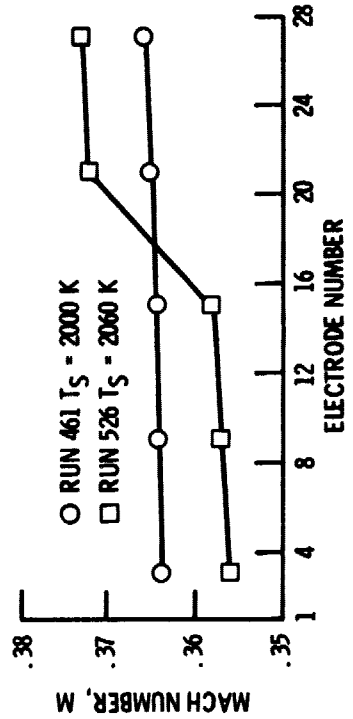


Figure 1. - Variation of the Mach number along the channel length.

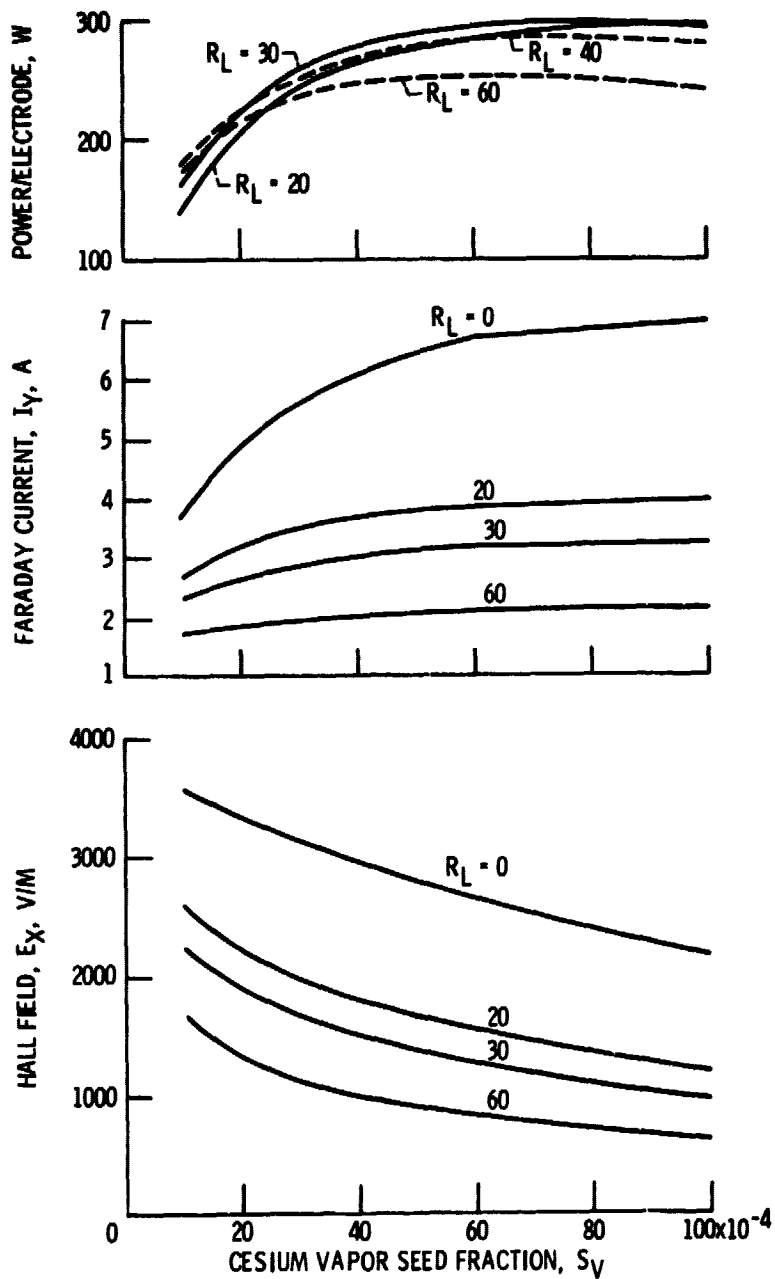


Figure 2. - Equilibrium power/electrode, current/electrode, and Hall field versus vapor seed fraction and load resistance. $T_S = 2060$ K, $M = 0.37$, $B = 1.8$ T

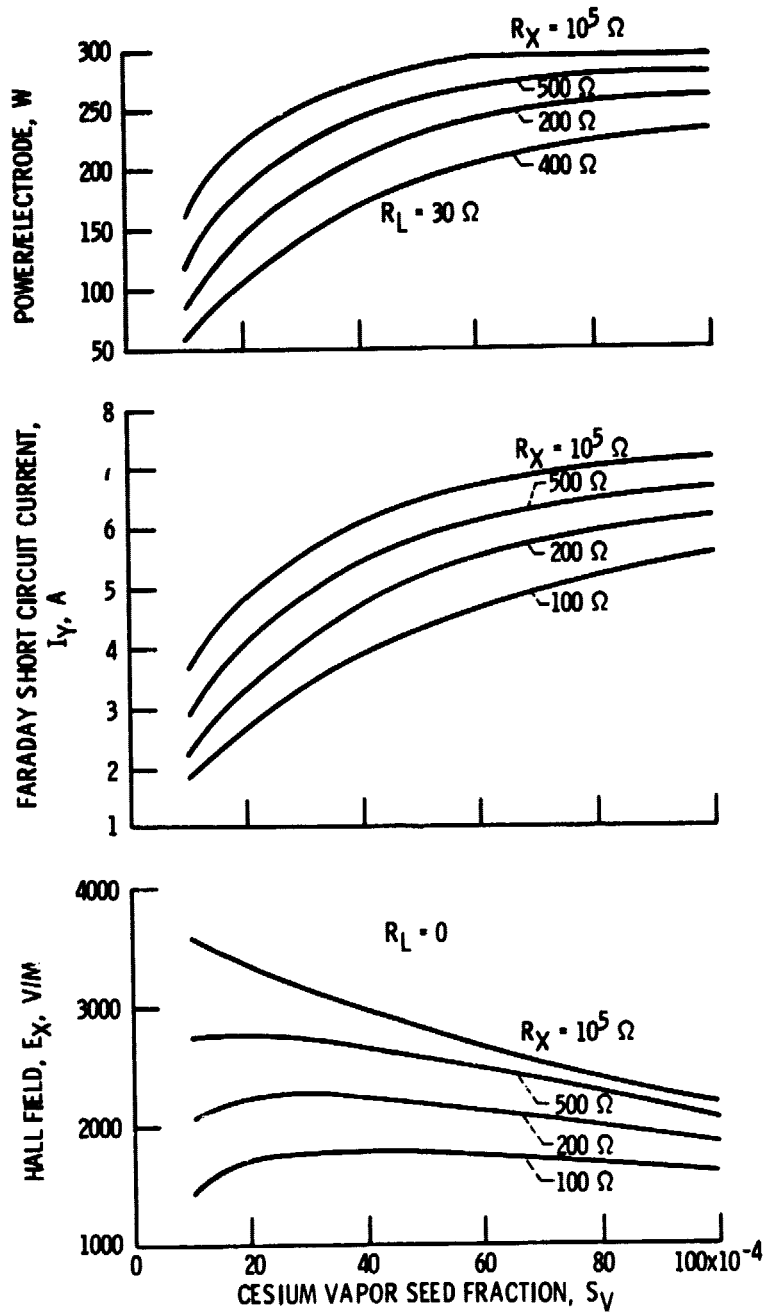


Figure 3. - Effect of Hall leakage resistance on ideal equilibrium performance.

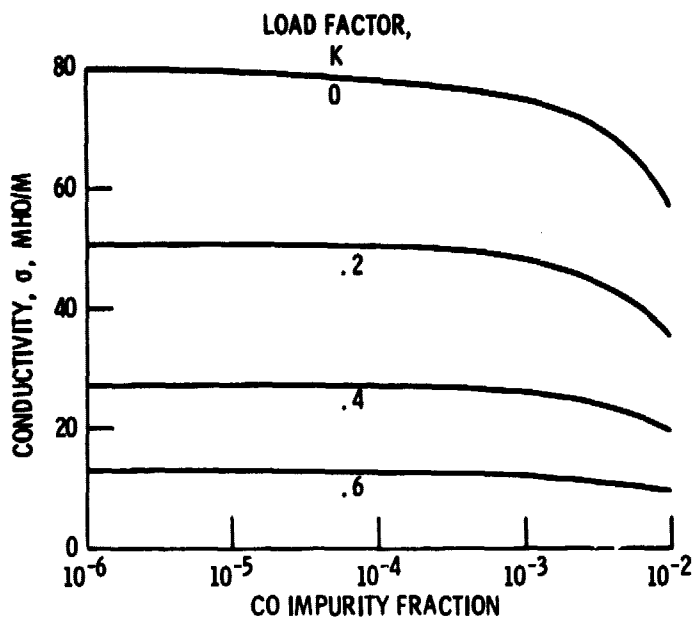


Figure 4. - Nonequilibrium electrical conductivity versus CO impurity fraction. $T_S = 2060$, $M = 0.37$, $B = 1.8$ T, $S_V = 0.005$

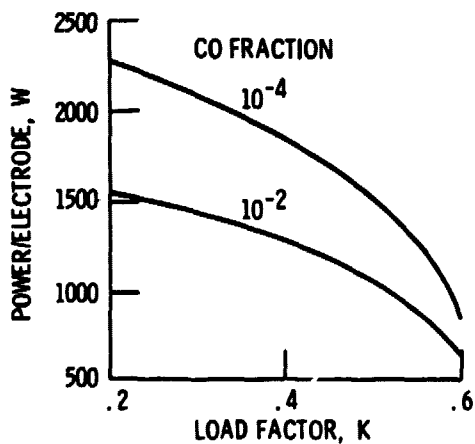


Figure 5. - Power per electrode versus load factor and CO fraction for nonequilibrium performance. $T_S = 2060$ K, $M = 0.37$, $B = 1.8$ T, $S_V = 0.005$

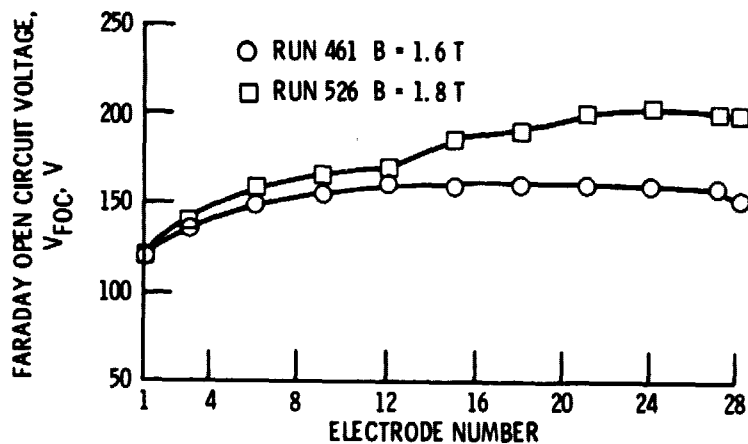


Figure 6. - Variation of Faraday open circuit voltage, V_{FOC} , along the channel length.

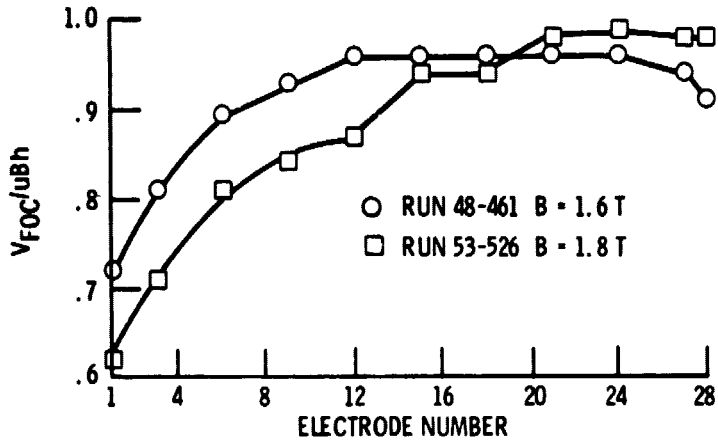


Figure 7. - Ratio of Faraday open circuit voltage to ideal V_{FOC}/uBh versus electrode position.

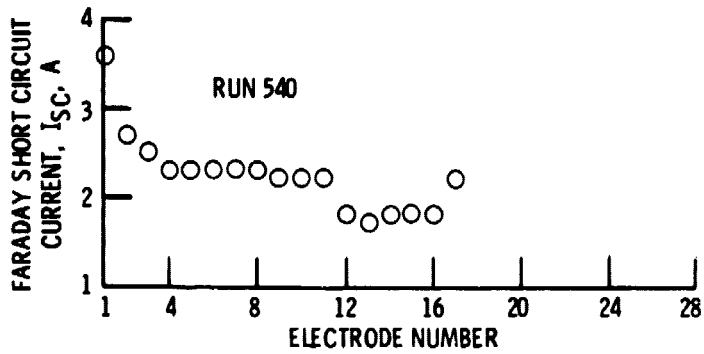


Figure 8. - Variation of short circuit current, I_{SC} , along the channel length.